

AD \_\_\_\_\_

Award Number: DAMD17-03-1-0251

TITLE: Rational Inhibitors of DNA Base Excision Repair (BER)  
Enzymes: New Tools for Elucidating the Role of the BER  
in Cancer Chemotherapy

PRINCIPAL INVESTIGATOR: Daniel J. Krosky

CONTRACTING ORGANIZATION: Johns Hopkins University School of Medicine  
Baltimore, MD 21205-2196

REPORT DATE: May 2005

TYPE OF REPORT: Annual Summary

PREPARED FOR: U.S. Army Medical Research and Materiel Command  
Fort Detrick, Maryland 21702-5012

DISTRIBUTION STATEMENT: Approved for Public Release;  
Distribution Unlimited

The views, opinions and/or findings contained in this report are those of the author(s) and should not be construed as an official Department of the Army position, policy or decision unless so designated by other documentation.

20050916 171

**REPORT DOCUMENTATION PAGE**Form Approved  
OMB No. 074-0188

Public reporting burden for this collection of information is estimated to average 1 hour per response, including the time for reviewing instructions, searching existing data sources, gathering and maintaining the data needed, and completing and reviewing this collection of information. Send comments regarding this burden estimate or any other aspect of this collection of information, including suggestions for reducing this burden to Washington Headquarters Services, Directorate for Information Operations and Reports, 1215 Jefferson Davis Highway, Suite 1204, Arlington, VA 22202-4302, and to the Office of Management and Budget, Paperwork Reduction Project (0704-0188), Washington, DC 20503

**1. AGENCY USE ONLY**  
(Leave blank)**2. REPORT DATE**  
May 2005**3. REPORT TYPE AND DATES COVERED**  
Annual Summary (21 Apr 2004 - 20 Apr 2005)**4. TITLE AND SUBTITLE**

Rational Inhibitors of DNA Base Excision Repair (BER)  
Enzymes: New Tools for Elucidating the Role of the BER in  
Cancer Chemotherapy

**5. FUNDING NUMBERS**  
DAMD17-03-1-0251**6. AUTHOR(S)**

Daniel J. Krosky

**7. PERFORMING ORGANIZATION NAME(S) AND ADDRESS(ES)**

Johns Hopkins University School of Medicine  
Baltimore, MD 21205-2196

**E-Mail:** Dkrosky1@jhmi.edu**8. PERFORMING ORGANIZATION  
REPORT NUMBER****9. SPONSORING / MONITORING  
AGENCY NAME(S) AND ADDRESS(ES)**

U.S. Army Medical Research and Materiel Command  
Fort Detrick, Maryland 21702-5012

**10. SPONSORING / MONITORING  
AGENCY REPORT NUMBER****11. SUPPLEMENTARY NOTES****12a. DISTRIBUTION / AVAILABILITY STATEMENT**

Approved for Public Release; Distribution Unlimited

**12b. DISTRIBUTION CODE****13. ABSTRACT (Maximum 200 Words)**

In this funding period we have completed Task 1 and 2 of the approved Statement of Work, which seek to develop useful inhibitor scaffolds for the DNA repair enzyme uracil DNA glycosylase (UDG) and determine their potency against human UDG. To these ends, we have rationally developed a potent DNA-based inhibitor and, through high throughput synthesis and screening, several small molecule inhibitors for human UDG. The small molecule inhibitors are expected to be cell permeable, and in conjunction with 5-fluorouracil, may have potential for anticancer therapy. This work has resulted in one publication during this funding period.

**14. SUBJECT TERMS**

Uracil DNA glycosylase, inhibitors, 5-fluorouracil, breast cancer

**15. NUMBER OF PAGES**

16

**16. PRICE CODE****17. SECURITY CLASSIFICATION  
OF REPORT**

Unclassified

**18. SECURITY CLASSIFICATION  
OF THIS PAGE**

Unclassified

**19. SECURITY CLASSIFICATION  
OF ABSTRACT**

Unclassified

**20. LIMITATION OF ABSTRACT**

Unlimited

## Table of Contents

Cover.....	1
SF 298.....	2
Table of Contents.....	3
Introduction.....	4
Body.....	4
Key Research Accomplishments.....	5
Reportable Outcomes.....	5
Conclusions.....	5
References.....	5
Appendices.....	6

## INTRODUCTION

This program seeks to obtain a fundamental understanding of the chemical mechanisms by which enzymes repair damaged DNA, and to use this information to design small molecule inhibitors of these enzymes. The driving force for these efforts is the recognition that the effectiveness of cancer chemotherapy regimes is intimately connected to, and in some cases directly relies on, DNA damage repair pathways. A more sophisticated understanding of the roles of DNA damage repair in the pharmacology of DNA replication inhibitors will allow for the design of better treatments against breast and other cancers.

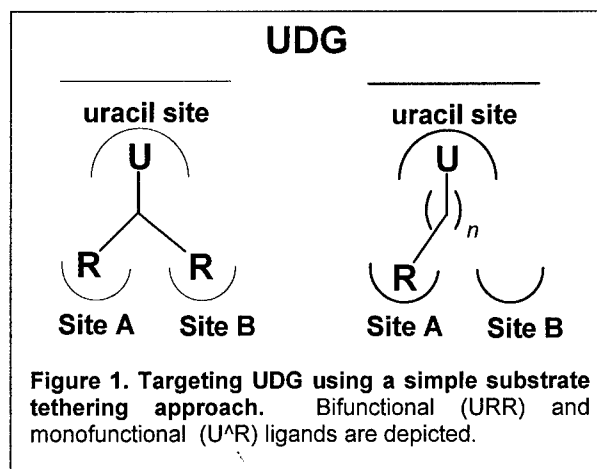
Studies during this period have focused on Task 1 and 2 in the original Statement of Work. We have explored how uracil DNA glycosylase (UDG) binds to substrate DNA with such high affinity, and have utilized this knowledge to synthesize a very tight binding DNA-based inhibitor of the enzyme. We also have used a new high throughput screen for UDG to identify inhibitors from a novel directed uracil library that we have constructed. This reporting period has produced one publication in a peer-reviewed journal and one more manuscript is in preparation.

## BODY

A major accomplishment of this funding period was the identification of the damaged DNA features that are important for high affinity binding by UDG. This work, which was published in the journal *Biochemistry* (see Appendix), revealed that tight binding DNA molecules could be constructed if the uracil substrate was presented to the enzyme in the context of a base pair that lacks hydrogen bonds and exhibits greater flexibility than normal DNA base pairs. Such designer uracil sites bind 43,000-fold more tightly than sites that lack these features.

Our new small molecule inhibitor development strategy uses the specificity and binding energy of the uracil ligand to target the UDG active site, and then relies upon random exploration of binding sites for tethered R groups (Fig. 1). Various types of tethering strategies are being pursued in the pharmaceutical industry and successful results in several systems have been reported. Our approach has the broader impact of exploring novel synthetic and screening strategies to discover inhibitors of enzymes that repair DNA. Such targets are largely unexplored in terms of their therapeutic potential.

This library is constructed by attaching one end of a bis-(aminooxy)alkane linker scaffold to C6, C5 and N1 aldehyde derivatives of uracil as shown in Fig. 2. The uracil-oximes may then be connected to a variety of aldehydes using the free ONH2 group on the linker. The bis-(aminooxy)alkane scaffold is ideal because it allows variation of the linker length to probe different potential binding surfaces on the enzyme (Fig. 2), and the



reactions go to completion negating the requirement for purification steps (see below). The potential size of the directed MF library may be estimated as ~ 4,500 compounds. This calculation assumes the reaction of ~300 random RCHO compounds X 3 uracil aldehyde derivatives X 5 linker lengths = 4,500 unique compounds.

## KEY RESEARCH ACCOMPLISHMENTS

- Elucidated the molecular determinants for high affinity binding of uracil-substrates by UDG and designed a high affinity DNA-based inhibitor (SOW, Task 1).
- Designed and screened a novel uracil-based small molecule library for inhibition of hUDG (SOW, Task 2).
- Identified and characterized several small molecule inhibitors of hUDG.

## REPORTABLE OUTCOMES:

This work has resulted in one published manuscript:

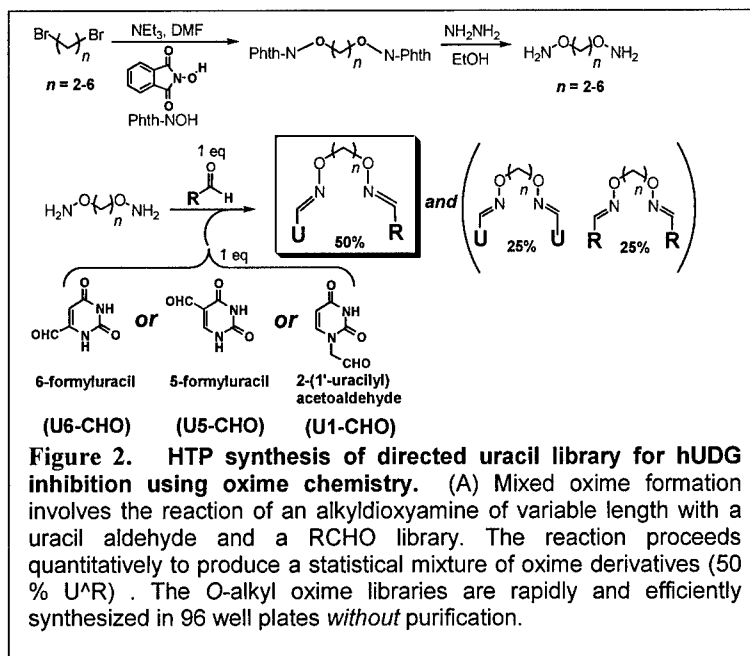
1. Krosky, D. J. and Stivers, J. T. (2005) The Origins of High Affinity Enzyme Binding to an Extrahelical DNA Base, *Biochemistry* **44**, 5949-5959.

## CONCLUSIONS:

The long-term goal of this research is to increase the effectiveness of 5-FU chemotherapy through the selective targeting of BER repair enzymes such as UDG. We have made significant progress towards this goal in this funding period through the synthesis of a very potent DNA-based inhibitor of the enzyme. We have also made significant progress towards the development of cell permeable small molecule inhibitors of UDG.

**REFERENCES:** None

**APPENDICES:** One manuscript is included (see above).



## Articles

---

### The Origins of High-Affinity Enzyme Binding to an Extrahelical DNA Base<sup>†</sup>

Daniel J. Krosky,<sup>‡</sup> Fenhong Song,<sup>§</sup> and James T. Stivers<sup>\*,‡</sup>

*Department of Pharmacology and Molecular Sciences, The Johns Hopkins School of Medicine, 725 North Wolfe Street, Baltimore, Maryland 21205-2185, and Center for Advanced Research in Biotechnology of the University of Maryland Biotechnology Institutes and the National Institute of Standards and Technology, 9600 Gudelsky Drive, Rockville, Maryland 20850*

*Received January 14, 2005; Revised Manuscript Received March 3, 2005*

**ABSTRACT:** Base flipping is a highly conserved strategy used by enzymes to gain catalytic access to DNA bases that would otherwise be sequestered in the duplex structure. A classic example is the DNA repair enzyme uracil DNA glycosylase (UDG) which recognizes and excises unwanted uracil bases from DNA using a flipping mechanism. Previous work has suggested that enzymatic base flipping begins with dynamic breathing motions of the enzyme-bound DNA substrate, and then, only very late during the reaction trajectory do strong specific interactions with the extrahelical uracil occur. Here we report that UDG kinetically and thermodynamically prefers substrate sites where the uracil is paired with an unnatural adenine analogue that lacks any Watson–Crick hydrogen-bonding groups. The magnitude of the preference is a striking 43000-fold as compared to an adenine analogue that forms three H-bonds. Transient kinetic and fluorescence measurements suggest that preferential recognition of uracil in the context of a series of incrementally destabilized base pairs arises from two distinct effects: weak or absent hydrogen bonding, which thermodynamically assists extrusion, and, most importantly, increased flexibility of the site which facilitates DNA bending during base flipping. A coupled, stepwise reaction coordinate is implicated in which DNA bending precedes base pair rupture and flipping.

Enzymes that modify or cleave nucleobases in DNA, such as DNA methyltransferases and DNA glycosylases, are confronted with a formidable chemical problem: gaining access to substrate bases that are sequestered inside the DNA double helix (1–3). A conserved enzymatic solution to this problem is base flipping, where the target base and sugar

are extruded from the DNA duplex into the enzyme active site (4).

Structural and mechanistic studies indicate that base flipping is a multistep process involving two coupled reaction coordinates (Figure 1A) (5–12), which are depicted using a free energy contour plot in Figure 1B. The first coordinate involves ~180° rotation of the entire target nucleotide from the duplex stack (vertical axis, Figure 1B), while the second coordinate involves enzyme-induced DNA bending (horizontal axis, Figure 1B). The progress along each reaction coordinate may be perfectly synchronized (diagonal dashed line, Figure 1B), or alternatively, one process may proceed ahead of the other (curved trajectory, Figure 1B). For instance, if DNA bending proceeds ahead of nucleotide

---

<sup>†</sup> This work was supported by National Institutes of Health Grant GM56834-10. D.J.K. was supported by the DOD Breast Cancer Research Program (DAMD17-03-1-1251).

\* To whom correspondence should be addressed. Tel: 410-502-2758. Fax: 410-955-3023. E-mail: jstivers@jhmi.edu.

<sup>‡</sup> The Johns Hopkins School of Medicine.

<sup>§</sup> Center for Advanced Research in Biotechnology of the University of Maryland Biotechnology Institutes and the National Institute of Standards and Technology.

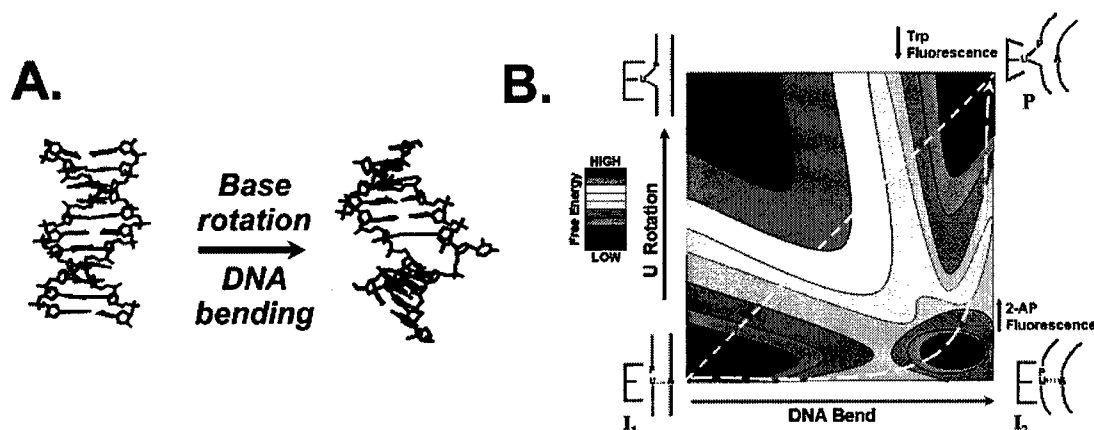


FIGURE 1: Uracil flipping has two coupled reaction coordinates involving base rotation and DNA bending. (A) Upon binding to free B DNA (left) UDG rotates the deoxyuridine nucleotide from the DNA base stack by  $180^\circ$  and bends the DNA by about  $40^\circ$ . The DNA structure on the right was extracted from the complex of UDG with substrate analogue DNA (PDB code 1EMH) (8). (B) A two-dimensional free energy contour map depicting the two coupled reaction coordinates of base rotation (vertical coordinate) and DNA bending (horizontal coordinate). The diagram shows the two enzyme-bound intermediates ( $I_1$ ,  $I_2$ ) that have been previously detected using rapid kinetic methods (5, 6) and the final product of the flipping and bending reaction ( $P$ ). In principle, progress along both reaction coordinates may be synchronized (diagonal line), or one process may lag behind the other. The contour map depicts the reaction trajectory (curved dashed line) where bending precedes flipping, and a low energy (blue) bent intermediate is formed before significant progress along the base rotation coordinate occurs ( $I_2$ ). Thus, flipping uracil from unbent DNA is a high-energy (red) improbable process (upper left corner). Formation of  $I_2$  can be followed using the increased fluorescence of the 2-aminopurine probe which is adjacent to the uracil and is very sensitive to base stacking (see Figure 2) (5, 6). Formation of  $P$  is discretely monitored by following the decrease in tryptophan fluorescence of UDG that accompanies base flipping (5, 6).

rotation, a bent intermediate may form (lower right corner, Figure 1B) before the hydrogen bonds to the target base are broken and the base is expelled into the enzyme active site (upper right corner, Figure 1B). A coupled reaction coordinate for base flipping suggests that if discrete alterations in the structural or dynamic features of the DNA substrate are made, then progress along one or both coordinates could be perturbed in a systematic way. This would allow a linear free energy perturbation (LFEP)<sup>1</sup> analysis analogous to that employed in simple chemical reactions involving coupled processes such as bond formation to a nucleophile and bond breakage to a leaving group (13).

A LFEP approach that we are continuing to explore for the DNA repair enzyme uracil DNA glycosylase (UDG) is to use DNA substrates in which the number of hydrogen bonds between the target uracil (U) and its opposing base (X) are systematically varied (Figure 2) (14). Our original hypothesis was that removal of base pair hydrogen bonds would thermodynamically facilitate uracil flipping and enzyme binding by destabilizing the uracil in the DNA base stack (i.e., by raising the free energy of the lower left corner of the reaction coordinate diagram in Figure 1B). A LFEP analysis has confirmed this initial expectation, where a strong linear correlation was found between the free energy of UDG binding to a series of DNA duplexes with increasingly destabilized U·X base pairs ( $m = -0.37$ ,  $R^2 = 0.86$ ) (14). A key question arising from this thermodynamic study is the mechanistic origin of the dramatically increased binding affinity to destabilized damaged sites.

Here we use a similar LFEP approach to correlate the effects of stepwise ablation of hydrogen bonds in the U·X

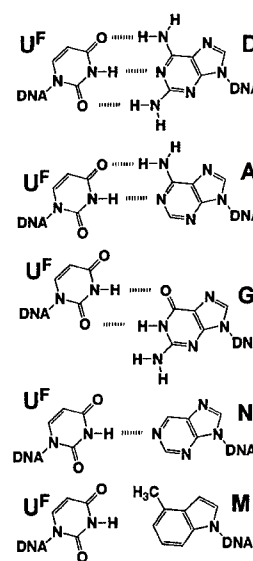
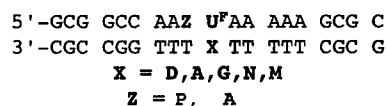


FIGURE 2: Sequences of 19-mer DNA substrates used in the kinetic studies and hydrogen-bonding structures of the U<sup>F</sup>·X base pairs based on the literature: U<sup>F</sup>·D (57, 58), U<sup>F</sup>·G (59), U<sup>F</sup>·N (47, 48), and U<sup>F</sup>·M (29). Abbreviations: M, 4-methylindole nucleotide; D, diaminopurine nucleotide; N, purine nucleotide; U<sup>F</sup>, 2'-β-fluoro-2'-deoxyuridine nucleotide.

base pair with the rate of base extrusion (nucleotide rotation reaction coordinate) and the rate of conformational changes in the DNA (bending reaction coordinate). To monitor the progress along these coordinates, we employ two indirect signal changes. The first follows the increase in fluorescence of a 2-aminopurine (2-AP) nucleotide adjacent to the target uracil (5). This signal is sensitive to the extent of stacking

<sup>1</sup> Abbreviations: LFEP, linear free energy perturbation; 2-AP, 2-aminopurine; FRET, fluorescence resonance energy transfer; M, 4-methylindole nucleotide; D, diaminopurine nucleotide; Y, pyrene nucleotide; N, purine nucleotide; Φ, tetrahydrofuran abasic nucleotide; U<sup>F</sup>, 2'-β-fluoro-2'-deoxyuridine nucleotide; UDG, uracil DNA glycosylase.

of 2-AP with the uracil (15, 16) and thus reports on conformational changes in the DNA as well as progress along the base rotation coordinate (6, 17–19). The second signal involves a decrease in UDG tryptophan fluorescence that accompanies a conformational change in UDG as it closes around the fully extrahelical uracil. This signal change has been shown by structural (8), kinetic (5, 6, 17, 20), and mutagenesis studies (6, 17) to correlate exclusively with formation of the final hydrogen-bonding and stacking interactions of the uracil base within the enzyme active site (i.e., formation of the final extrahelical state depicted in the upper right corner of Figure 1B). These studies suggest a base flipping pathway in which DNA bending precedes base rotation, thereby opening an unhindered passage by which uracil may exit the duplex. Surprisingly, binding studies of both rigid and flexible DNA duplexes indicate that a large amount of enzyme binding energy is consumed during the process of DNA bending. This finding appears to be a general feature of base flipping enzymes and is consistent with previous suggestions based on structural and biochemical observations with UDG as well as other base flipping enzymes (2, 21–27). Accordingly, strong binding of UDG to flexible target sites results not only from weakened hydrogen bonding of the uracil but also because flexible sites require less enzyme binding energy to bend. These unique features of target site recognition by UDG may be shared by other base flipping enzymes (28).

## EXPERIMENTAL PROCEDURES

**Materials.** The 2'-deoxynucleoside phosphoramidites, CPG supports, and DNA synthesis reagents were purchased from Glen Research (Sterling, VA), except for 2'- $\beta$ -fluoro-2'-deoxyuridine ( $U^F$ ), 4-methylindole nucleoside (M), and pyrene nucleoside (Y), which were synthesized as described previously (5, 29, 30). The oligonucleotides were synthesized using standard phosphoramidite chemistry on an Applied Biosystems 392 synthesizer. The oligonucleotides were purified by anion-exchange HPLC (Zorbax Oligo), followed by C-18 reversed-phase HPLC (Phenomenex Aqua column). Fractions containing pure oligonucleotide were concentrated to dryness in vacuo, redissolved in MilliQ water, and stored at  $-20^\circ\text{C}$ . The purity of the oligonucleotides was assessed by matrix-assisted laser desorption mass spectroscopy and denaturing polyacrylamide gel electrophoresis. The concentration of each oligonucleotide was determined using its extinction coefficient at 260 nm (31). DNA duplexes were hybridized in 10 mM Tris-HCl (pH 8.0) and 60 mM NaCl as described previously (5). The purification of *Escherichia coli* UDG has been described previously (32).

**$K_D$  Measurements.** The  $K_D$  values for binding of the  $U^F \cdot X$  duplexes to UDG were measured using a kinetic competitive inhibition fluorescence assay under conditions where the apparent  $K_i$  is equal to the  $K_D$  value (i.e.,  $[S] \ll K_m$ , where S exhibits rapid equilibrium binding). Reaction mixtures (148.5  $\mu\text{L}$ ) containing 10 mM Tris-HCl (pH 8.0), 60 mM NaCl, 12.5  $\mu\text{g/mL}$  BSA, 2  $\mu\text{M}$  AUPA substrate, and a variable amount of the  $U^F \cdot X$  duplex were placed in a 0.3 cm quartz cuvette, and its fluorescence emission at 370 nm was monitored every 10 s at  $25^\circ\text{C}$  on a SPEX FluoroMax-3 fluorometer ( $\lambda_{\text{ex}} = 320 \text{ nm}$ ) until the signal stabilized. UDG (1.5  $\mu\text{L}$ ) was then added to the reaction mixture to give a final concentration of 0.25 nM. The progress of the reaction

was then monitored as described above for 5 min. The  $K_D$  for each duplex was determined by fitting to the equation

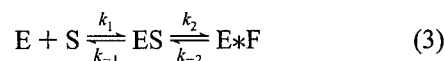
$$k_i/k_0 = 1/(1 + [U^F \cdot X]/K_D) \quad (1)$$

where  $k_i$  is the inhibited rate and  $k_0$  is the rate in the absence of competitor DNA.

**Stopped-Flow Fluorescence.** The observed rate constants for the formation of UDG-DNA complexes were measured on an Applied Photophysics 720 stopped-flow fluorometer (Surrey, U.K.). All measurements were performed under pseudo-first-order conditions where the concentration of the unlabeled component was at least 4-fold greater the concentration of the labeled species. All measurements were made using a buffer containing 10 mM Tris-HCl (pH 8.0), 60 mM NaCl, and 1 mM DTT. For experiments where changes in 2-AP fluorescence were observed, excitation was at 315 nm, and a 360 nm long-pass emission filter was used. In experiments where tryptophan fluorescence was measured, an excitation wavelength of 290 nm was used with a 335 nm long-pass emission filter. All kinetic traces were well fitted to a first-order rate expression to obtain the observed rate constant ( $k_{\text{obsd}}$ , eq 2).

$$F_t = \Delta F \exp(1 - k_{\text{obsd}}t) + F_0 \quad (2)$$

For the experiments in which the rate of 2-AP signal increase of the DNA was monitored, a solution containing a variable amount of UDG was rapidly mixed with a fixed concentration of 2-AP-labeled DNA. Final concentrations of enzyme and DNA after mixing were in the range 0.4–6.4  $\mu\text{M}$  and 100 nM, respectively. For the experiments in which the rate of tryptophan signal decrease of the enzyme was monitored, a solution containing a variable amount of DNA was rapidly mixed with a fixed concentration of the enzyme. In these experiments, the final concentrations of DNA and enzyme after mixing were in the range 0.4–12.8  $\mu\text{M}$  and 100 nM, respectively. Measurements with the  $U^F \cdot M$  duplex using 2-AP fluorescence could not be accurately made above 1.6  $\mu\text{M}$  because only 20% of the observable signal remained after the  $\sim 1$  ms dead time of the instrument had elapsed. As previously observed, plots of  $k_{\text{obsd}}$  against  $[\text{UDG}]$  or  $[U^F \cdot X]$  were hyperbolic, indicating a multistep binding mechanism. The kinetic parameters were extracted by fitting the data to a minimal two-step binding model (eqs 3 and 4),



$$k_{\text{obsd}} = \frac{k_{\text{off}}[S] + k_{\text{off}}}{K'[S] + 1} \quad (4)$$

where  $K' = k_1/(k_{-1} + k_{\text{max}})$  is the apparent affinity constant,  $k_{\text{on}} = K'(k_2 + k_{-2})$  is the apparent second-order association rate constant, and  $k_{\text{off}} = k_{-1}k_{-2}/(k_{-1} + k_2 + k_{-2})$  is the overall dissociation rate constant. The maximum rate constant for the unimolecular rearrangements detected by the 2-AP and tryptophan fluorescence signals is measured by the asymptote  $k_{\text{max}}^{2\text{AP}}$  (or  $k_{\text{max}}^{\text{Trp}} = k_2 + k_{-2}$ ) (5). Although base flipping has been previously shown to involve two internal steps rather than the one shown in eq 3 (6, 17, 20), the simplified analytical expression of eq 4 is very useful for comparing



the kinetic behavior of a series of substrates or mutated enzymes (6).

Very slow dissociation rate constants determined from the concentration dependence of  $k_{\text{obsd}}$  (eq 3) have a high degree of uncertainty because  $k_{\text{off}}$  is derived from the y-intercept of a plot of  $k_{\text{obsd}}$  against [S]. Under such conditions, a trapping experiment is required to obtain a more precise value for  $k_{\text{off}}$ . Trapping experiments for the substrates containing D, A, G, and N in the base pair with uracil were performed by rapidly mixing a solution consisting of UDG (200–500 nM) and 2-AP-labeled DNA (200 nM) with a large molar excess of nonfluorescent trapping duplex (20  $\mu$ M AU<sup>F</sup>A-11) (6) using a stopped-flow fluorometer. The time-dependent decrease in 2-AP fluorescence as the bound DNA irreversibly dissociated was fit to a single-exponential decay to obtain  $k_{\text{off}}$  (eq 5). Because of the very slow dissociation of U<sup>F</sup>•M,

$$F_t = \Delta F \exp(-k_{\text{off}}t) + F_0 \quad (5)$$

its  $k_{\text{off}}$  was measured by manually mixing a solution consisting of UDG (100 nM) and PU<sup>F</sup>•M (100 nM) with 1  $\mu$ M high-affinity trap, AU<sup>F</sup>A/TMT-15 (14). This reaction was performed using a 0.3 cm path length quartz cuvette (150  $\mu$ L) and a Spex FluoroMax-3 fluorometer. The time-dependent decrease in 2-AP emission at 370 nm was followed with excitation at 315 nm.

## RESULTS

**Binding of UDG to Destabilized Damaged Sites.** We synthesized a series of 19-mer DNA duplexes containing a series of U<sup>F</sup>•X base pairs using a sequence based on a duplex previously used in rapid kinetic studies of base flipping by UDG (Figure 2) (5). The 2' fluorinated deoxyuridine substrate analogue (U<sup>F</sup>) is an extremely slow substrate for UDG ( $t_{1/2} \sim 1$  day), allowing measurements of DNA binding and base flipping without the complication of glycosidic bond cleavage (5). The affinity of UDG for these duplexes was measured using a competitive inhibition kinetic assay (14). As previously observed for a series of 15-mer duplexes with a different sequence (14), the  $K_D$  values for the 19-mers decreased incrementally as the U<sup>F</sup>•X base pair weakened (Figure 3A and Table 1). The U<sup>F</sup>•M duplex, which contains no hydrogen bonds, binds a striking  $\sim 43400$ -fold (6.3 kcal/mol) more strongly than the duplex containing the U<sup>F</sup>•D base pair with three hydrogen bonds. Of note, the incremental decrease in the free energy of binding was only about 1 kcal/mol when the first and second hydrogen bonds were removed from the U<sup>F</sup>•D base pair (Figure 3B), which is similar to estimates of the free energy contribution of individual hydrogen bonds to the stability of duplex nucleic acids (33). In contrast, removal of the last hydrogen bond to form the U<sup>F</sup>•M pair resulted in a much larger 4 kcal/mol decrease in binding free energy, indicating the presence of additional energetic contributions. These additional contributions may involve a loss of both hydrogen bond and base stacking interactions, leading to a large increase in conformational entropy of the U<sup>F</sup>•M base pair (14). This result suggests that, with respect to the free energy of binding, increased flexibility of the site may play a more important role than the enthalpic benefit of removing single hydrogen bonds (see below).

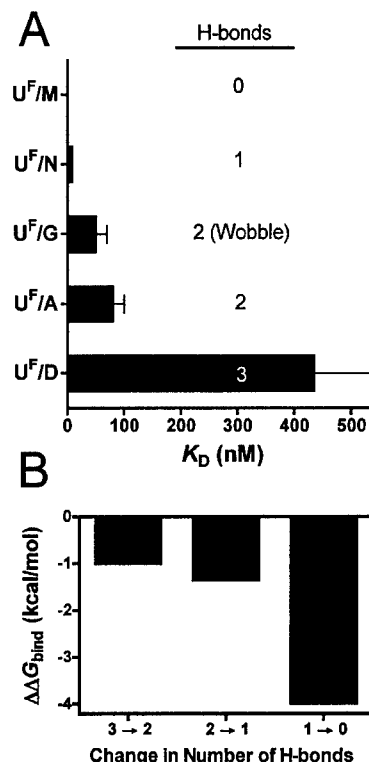


**Figure 3**

FIGURE 3: Binding affinities of UDG for U<sup>F</sup>•X DNA duplexes and incremental change in binding free energy when each hydrogen bond is removed. (A) Trend in dissociation binding constants as base pair hydrogen bonds are removed (see also Table 1). The number of hydrogen bonds in the U<sup>F</sup>•X base pair is shown to the right of the bars. (B) Incremental change in binding free energy as each hydrogen bond is removed from the U<sup>F</sup>•X base pair ( $\Delta\Delta G_{\text{bind}} = -RT \ln K_D^n/K_D^{n-1}$ , where  $n$  is the number of hydrogen bonds in the base pair).

**Binding Kinetics.** To dissect the origins of the dramatically enhanced binding affinity of the duplexes with destabilized U<sup>F</sup>•X base pairs, the kinetics of association and dissociation were measured. Association rates were measured using stopped-flow fluorescence measurements by monitoring either the increase in 2-AP fluorescence that accompanies uracil unstacking and DNA bending (Figure 4A) or the decrease in tryptophan fluorescence that marks the attainment of the final extrahelical state (Figure 4B) (5, 6, 17). As observed in previous studies using duplexes with U<sup>F</sup>•A and U<sup>F</sup>•G base pairs (5), plots of  $k_{\text{obsd}}$  versus concentration were hyperbolic when either the 2-AP or tryptophan fluorescence signals were monitored (panels A and B of Figure 5, respectively). This kinetic behavior indicates a change in rate-limiting step from bimolecular encounter at low concentrations of the varied reactant to a unimolecular conformational change of the DNA and enzyme at high reactant concentrations. All hyperbolic plots were fit to the two-step binding model (eq 4), and the kinetic constants obtained from this analysis are reported in Table 1.

There are revealing aspects of the kinetics for the 2-AP and tryptophan fluorescence changes. First, for the substrate with the most stable base pair (U<sup>F</sup>•D), the association kinetics measured using the 2-AP signal ( $k_{\text{on}}^{2\text{AP}}$ ) is 3-fold faster than when the tryptophan signal is followed ( $k_{\text{on}}^{\text{TTP}}$ ) (Table 1).

Table 1: Binding Affinities and Kinetic Parameters for UDG Association and Dissociation with U<sup>F</sup>·X Duplexes

duplex	$K_D$ (nM)	$K'_{2AP}$ ( $\mu\text{M}^{-1}$ )	$K'^{\text{Trp}}$ ( $\mu\text{M}^{-1}$ )	$k_{\text{on}}^{2AP}$ ( $\mu\text{M}^{-1}\cdot\text{s}^{-1}$ )	$k_{\text{on}}^{\text{Trp}}$ ( $\mu\text{M}^{-1}\cdot\text{s}^{-1}$ )	$k_{\text{off}}$ ( $\text{s}^{-1}$ )	$K_D^{\text{calc}}$ (nM) <sup>d</sup>
U <sup>F</sup> ·D	434 ± 100 <sup>a</sup>	0.29 ± 0.05	0.12 ± 0.02	206 ± 22	72 ± 7	44 ± 1.3	214 ± 24
U <sup>F</sup> ·A	80 ± 20 <sup>a,b</sup>	0.08 ± 0.01	0.13 ± 0.01	236 ± 10	172 ± 8	26 ± 0.3	110 ± 4
U <sup>F</sup> ·G	50 ± 20 <sup>a,b</sup>	0.10 ± 0.01	0.25 ± 0.08	292 ± 13	331 ± 56	6.9 ± 0.04	24 ± 1
U <sup>F</sup> ·N	8.2 ± 0.3 <sup>c</sup>	0.20 ± 0.04	0.14 ± 0.01	282 ± 28	315 ± 5	6.0 ± 0.05	21 ± 2 <sup>c</sup>
U <sup>F</sup> ·M	0.01 ± 0.002 <sup>c</sup>	0.32 ± 0.15	0.64 ± 0.08	292 ± 40	666 ± 45	0.018 ± 0.001	0.062 ± 0.009 <sup>c</sup>

<sup>a</sup>  $K_D$  was determined by directly monitoring binding of DNA to UDG using 2-AP fluorescence (see Experimental Procedures). <sup>b</sup> Values previously reported (5). <sup>c</sup>  $K_D$  was determined using competitive inhibition assay with AU<sup>F</sup>·X substrate (see Experimental Procedures). The affinity of AU<sup>F</sup>·A is 2-fold greater than that of PU<sup>F</sup>·A (17). <sup>d</sup>  $K_D$  calculated from  $k_{\text{off}}/k_{\text{on}}^{2AP}$ .

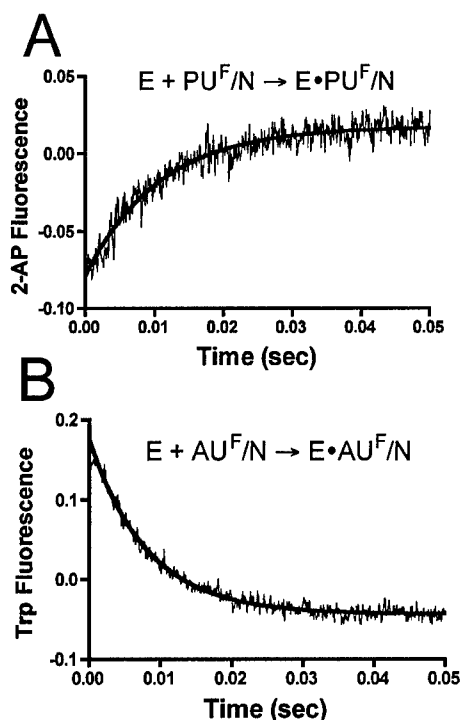


FIGURE 4: Stopped-flow fluorescence kinetic measurements of UDG association with U<sup>F</sup>·X duplex DNA. (A) Approach to equilibrium association rate of PU<sup>F</sup>·N (0.1  $\mu\text{M}$ ) and UDG (0.4  $\mu\text{M}$ ) monitored by the increase in 2-AP fluorescence. (B) Approach to equilibrium association rate of UDG (0.1  $\mu\text{M}$ ) and AU<sup>F</sup>·N (0.4  $\mu\text{M}$ ) monitored by the decrease in tryptophan fluorescence of UDG.

However, as hydrogen bonds are removed from the base pair  $k_{\text{on}}^{2AP}$  and  $k_{\text{on}}^{\text{Trp}}$  become indistinguishable. This result arises because  $k_{\text{on}}^{2AP}$  is nearly invariant across the whole series of duplexes, while  $k_{\text{on}}^{\text{Trp}}$  increases by about 9-fold (Figure 5C).<sup>2</sup> The observation that  $k_{\text{on}}^{\text{Trp}}$  is slower than  $k_{\text{on}}^{2AP}$  when the base pair is strong requires that the conformational change in the enzyme lags behind the structural perturbation in the DNA that results in the 2-AP fluorescence increase. The strong dependence of  $k_{\text{on}}^{\text{Trp}}$  on base pair hydrogen bonding indicates that these hydrogen bonds are broken very late

<sup>2</sup> The asymptotic  $k_{\text{obsd}}$  values for the 2-AP signal ( $k_{\text{max}}^{2AP} = k_2^{2AP} + k_{-2}^{2AP}$ ; see eq 3) increase by about 2-fold between U<sup>F</sup>·D and the U<sup>F</sup>·A or U<sup>F</sup>·G substrates but then decrease from these peak values by about 2-fold for the U<sup>F</sup>·N and U<sup>F</sup>·M substrates. This behavior may be qualitatively understood using the simplified two-step kinetic analysis we have employed. That is,  $k_2^{2AP}$  and  $k_{-2}^{2AP}$  are complex rate constants that reflect the interconversion of I<sub>1</sub>, I<sub>2</sub>, and P on the enzyme:  $k_{\text{max}}^{2AP}$  first increases as the conversion of I<sub>2</sub> → P becomes more rapid due to hydrogen bond ablation and then decreases because the reverse rate ( $k_{-2}^{2AP}$ ) becomes negligible for the U<sup>F</sup>·N and U<sup>F</sup>·M substrates due to stabilization of I<sub>2</sub> and P (i.e.,  $k_{\text{max}}^{2AP} \sim k_2^{2AP}$ ; see Discussion).

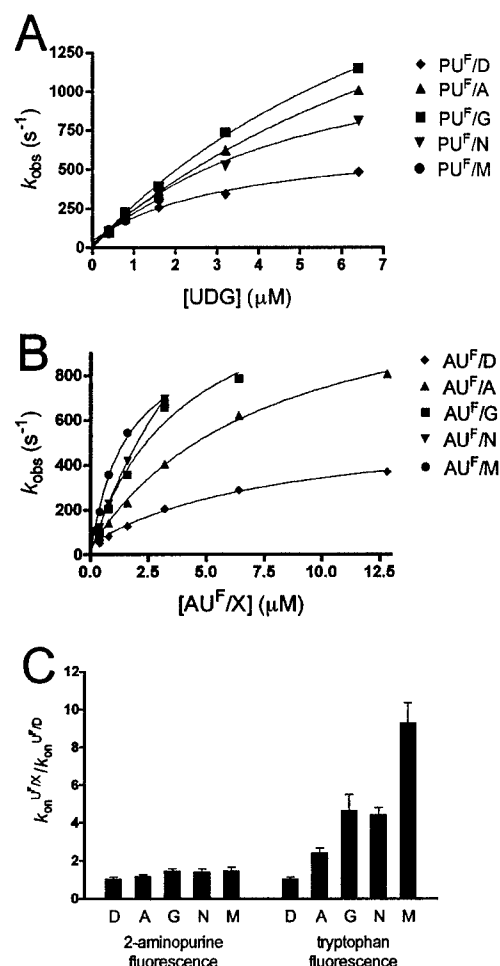


FIGURE 5: Concentration dependence of the apparent association rate constants ( $k_{\text{obs}}$ ) for the five different U<sup>F</sup>·X base pairs and relative  $k_{\text{on}}$  values as compared to the U<sup>F</sup>·D substrate. (A) Dependence of  $k_{\text{obs}}$  on the concentration of UDG followed by changes in 2-AP fluorescence. Data were fit to the two-step kinetic model (eqs 3 and 4). (B) Dependence of  $k_{\text{obs}}$  on the concentration of DNA followed by changes in Trp fluorescence. Data were fit to the two-step kinetic model (eqs 3 and 4). (C) Effect of changing U<sup>F</sup>·X base pair strength on  $k_{\text{on}}$ , expressed as the ratio of  $k_{\text{on}}(\text{U}^{\text{F}}\cdot\text{X})$  to  $k_{\text{on}}(\text{U}^{\text{F}}\cdot\text{D})$ . Ratios determined from the kinetics of the 2-AP and tryptophan fluorescence changes are displayed separately.

along the reaction coordinate, *after* the step that is reported on by the 2-AP signal and *during* the final conformational step when the enzyme closes around the uracil base. This result implies that the 6-fold 2-AP signal increase reflects the formation of an intermediate (I<sub>2</sub>, Figure 1) in which the uracil stacking interactions with the adjacent 2-AP base are perturbed, but the uracil retains hydrogen bonding with its

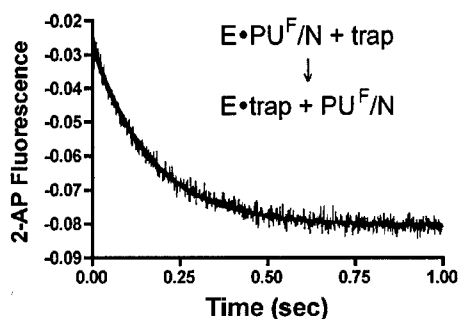


FIGURE 6: Determination of  $k_{\text{off}}$  using a trapping experiment. A complex of  $\text{PU}^{\text{F}}\cdot\text{N}$  ( $0.20\ \mu\text{M}$ ) and UDG ( $0.25\ \mu\text{M}$ ) was rapidly mixed with a large excess of nonfluorescent AUF $\cdot$ A-11 single-stranded DNA ( $20\ \mu\text{M}$ ) (6). The  $k_{\text{off}}$  is determined from fitting the time-dependent decrease in the 2-AP fluorescence of  $\text{PU}^{\text{F}}\cdot\text{N}$  as it is irreversibly released from UDG (eq 5).

partner base (6, 17). Since the preceding intermediate ( $\text{I}_1$ , Figure 1) is not detectably bent (7), and the subsequent extrahelical state is bent by about  $40^\circ$  (8), then the structural implication of the increase in 2-AP fluorescence is that the DNA is bent in the transition state leading to  $\text{I}_2$ ,<sup>3</sup> although the magnitude of the bending at this point along the reaction coordinate is not known. It is important to point out that the 9-fold increase in  $k_{\text{on}}$  pales in comparison with the approximately 43000-fold increase in UDG binding affinity when these three hydrogen bonds are ablated. Thus, the vast majority of the binding affinity increase is not attributable to  $k_{\text{on}}$ .

The above results strongly suggest that the large thermodynamic benefit of removing hydrogen bonds in the  $\text{U}^{\text{F}}\cdot\text{X}$  base pair arises from profound differences in the dissociation rates of these duplexes. To establish this point, the dissociation rates ( $k_{\text{off}}$ ) were measured using an irreversible trapping experiment (5) in which a solution of  $\text{UDG}\cdot(\text{PU}^{\text{F}}\cdot\text{X})$  was rapidly mixed with a large excess of unlabeled trapping DNA, and the decrease in the 2-AP signal was followed (Figure 6). The dissociation rate constants are reported in Table 1 and are consistent with the  $y$ -intercepts ( $k_{\text{off}}$ ) estimated from the concentration dependence of the association rates in Figure 5A,B. The dissociation rates were strongly dependent on the nature of the  $\text{U}^{\text{F}}\cdot\text{X}$  base pair, decreasing by over 4 orders of magnitude over the entire series, with  $k_{\text{off}}(\text{U}^{\text{F}}\cdot\text{D}) = 44\ \text{s}^{-1}$  and  $k_{\text{off}}(\text{U}^{\text{F}}\cdot\text{M}) = 0.018\ \text{s}^{-1}$ . These data provide strong evidence that removal of target base pair hydrogen bonds leads to profound stabilization of one or more enzyme-bound species on the uracil flipping pathway. Since the kinetic effect of removing hydrogen bonds appears very late during the uracil flipping process (i.e., during the

<sup>3</sup> We were unable to detect DNA bending by UDG employing standard fluorescence resonance energy transfer (FRET) methods and DNA substrates with fluorescence donor and acceptor groups on each end (51, 52). We attribute this result to interaction of the rhodamine fluorophore with binding sites in the free DNA (53, 54), which may be disrupted when the enzyme binds, resulting in no FRET change. Based on crystallographic models of bent DNA bound to UDG (not shown), we would have expected a substantial 1.4-fold FRET increase. The same negative result was obtained when the donor or acceptor was placed on the 3' or 5' end of the uracil-containing strand or when a 15-mer or 19-mer duplex was used. We note that an unexpected and small 15% FRET decrease was recently reported for *EcoRI* methyltransferase which also flips a DNA base by a putative bending mechanism, although an increase was expected (55). We conclude that FRET results should be interpreted cautiously in base flipping systems.

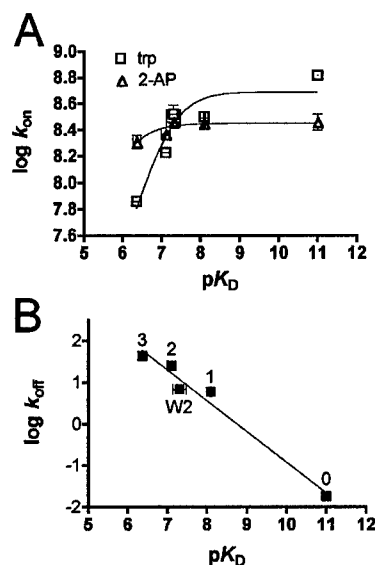


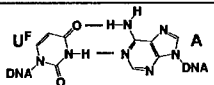
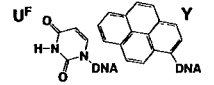
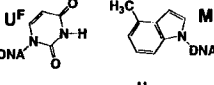
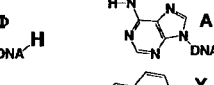
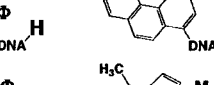
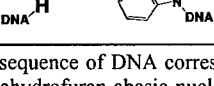
FIGURE 7: Logarithmic dependences of  $k_{\text{on}}$  and  $k_{\text{off}}$  on the binding affinity of UDG for  $\text{U}^{\text{F}}\cdot\text{X}$  DNA ( $\text{pK}_{\text{D}}$ ). (A) Logarithmic dependence of  $k_{\text{on}}$  on  $\text{pK}_{\text{D}}$ . The data were fit to the empirical equation  $\log k_{\text{on}} = \log k_{\text{diff}} - \log(1 + 10^{\text{pK}_0 - \text{pK}_{\text{D}}})$ , where  $k_{\text{diff}}$  is the rate constant for diffusional encounter and  $\text{pK}_0$  is an empirical constant. (B) Linear dependence of  $\log k_{\text{off}}$  on binding affinity (slope =  $0.74 \pm 0.07$ ,  $R^2 = 0.97$ ). For reference, the number of hydrogen bonds in each destabilized  $\text{U}^{\text{F}}\cdot\text{X}$  base pair is indicated above each data point.

last conformational step monitored by tryptophan fluorescence; see above), then the stabilized species must be one or both of the complexes shown in the upper and lower right-hand corners of Figure 1B ( $\text{I}_2$ ,  $\text{P}$ ).

**Linear Free Energy Correlations.** The quantitative dependence of  $k_{\text{on}}$  and  $k_{\text{off}}$  on UDG binding affinity provides further insights into the mechanistic basis for the enhanced binding of duplexes with destabilized base pairs. A plot of  $\log k_{\text{on}}^{2\text{AP}}$  versus  $\text{pK}_{\text{D}}$  is nearly flat across the whole series (Figure 7A, triangles) with an average value  $k_{\text{on}} = 2.8 \times 10^8\ \text{M}^{-1}\ \text{s}^{-1}$  indicative of near diffusion-controlled binding except for the substrate with the most stable base pair ( $\text{U}^{\text{F}}\cdot\text{D}$ ) which falls slightly below this average value. Thus, all internal kinetic steps preceding and including the 2-AP fluorescence change are rapid as compared to the encounter rate. In contrast,  $k_{\text{on}}^{\text{Trp}}$  shows a linear increase as a function of  $\text{pK}_{\text{D}}$  for the more stable  $\text{U}^{\text{F}}\cdot\text{D}$  and  $\text{U}^{\text{F}}\cdot\text{A}$  duplexes, followed by downward curvature to a plateau value of  $k_{\text{on}}^{\text{Trp}} = 4 \times 10^8\ \text{M}^{-1}\ \text{s}^{-1}$  for the most destabilized base pairs (Figure 7A, squares). This behavior indicates a change in rate-limiting step as a function of base pair stability from the step giving rise to the tryptophan fluorescence change to that involving diffusion-controlled encounter. We conclude that the thermodynamic stability of the  $\text{U}^{\text{F}}\cdot\text{X}$  base selectively alters the activation barrier for the step reported by  $k_{\text{on}}^{\text{Trp}}$ .

In contrast with  $\log k_{\text{on}}$ , there is a linear dependence of  $\log k_{\text{off}}$  on  $\text{pK}_{\text{D}}$ , with the dissociation rate decreasing steeply as UDG affinity increases (Figure 7B). From the slope of this correlation ( $-0.74 \pm 0.07$ ), it can be inferred that about 74% of the difference in binding energies between any two  $\text{U}^{\text{F}}\cdot\text{X}$  duplexes arises from  $k_{\text{off}}$ . The simplest mechanism that accounts for the small effect of base pair strength on  $k_{\text{on}}$ , and the large effect on  $k_{\text{off}}$ , is the progressive stabilization of one or more enzyme-bound species as hydrogen bonds are removed (see Discussion).

Table 2: Effect of Pyrene Nucleoside on Binding Affinity of UDG to Uracil and the Abasic Site Containing DNA<sup>a</sup>

Duplex DNA	$K_D$ (nM)
	$300 \pm 50$
	$120 \pm 30$
	$0.24 \pm 0.03$
	$100 \pm 10$
	$8700 \pm 675$
	$18 \pm 3.0$

<sup>a</sup> The sequence of DNA corresponds to 15-mer duplexes in ref 14.  $\Phi$  = tetrahydrofuran abasic nucleotide analogue.

**Base Pair Hydrogen Bonds, DNA Flexibility, and UDG Binding.** To test the role of DNA flexibility on binding affinity, we employed a novel structure-reactivity approach. This strategy takes advantage of the decrease in flexibility of the target site when it is modified with a rigid pyrene nucleotide on one strand (Table 2) (17, 30, 34–36). We originally used a uracil-pyrene base pair ( $U^F \cdot Y$ ) to preorganize uracil in an extrahelical conformation (34), with the rationale that the planar aromatic ring structure of pyrene would fully encompass the entire volume normally occupied by the standard  $U^F \cdot A$  base pair, thereby presenting the uracil to the enzyme in an extrahelical conformation that favors binding (i.e., the energetic penalty for uracil flipping is prepaid, allowing for tighter binding). In accord with this reasoning, DNA that contained a  $U^F \cdot Y$  pair fully rescued the catalytic and base flipping activities of UDG mutants that were incapable of pushing uracil from the DNA base stack in the context of a  $U^F \cdot A$  base pair (17, 34).

Although base flipping mutants showed dramatic increases in their site-specific binding affinity and catalytic activity when a  $U^F \cdot Y$  pair was used, wild-type UDG bound with nearly equal affinity to DNA containing either a  $U^F \cdot Y$  or  $U^F \cdot A$  base pair (34). This finding is reaffirmed in Table 2 where the binding affinity of UDG to a 15-mer duplex containing a  $U^F \cdot A$  and  $U^F \cdot Y$  pair is shown to differ by only 2.5-fold. This result is in dramatic contrast to the 1200-fold tighter binding of the  $U^F \cdot M$  duplex as compared to  $U^F \cdot A$  using the same 15-mer context (Table 2). These observations indicate that there is a cryptic energetic penalty for binding of the  $U^F \cdot Y$  duplex that is not present for binding of the  $U^F \cdot M$  duplex even though  $U^F \cdot M$  and  $U^F \cdot Y$  both lack hydrogen bonds to the uracil base. Thus a key question is the basis for the dramatically tighter binding of the  $U^F \cdot M$  duplex as compared to  $U^F \cdot Y$  ( $\Delta\Delta G = 3.7$  kcal/mol).

A likely explanation is that the pyrene nucleoside serves to stiffen the DNA at the apex of the bend induced during base flipping and thus requires a greater expenditure of

binding energy by UDG in order to distort the DNA as compared to  $U^F \cdot M$ . This idea is consistent with previous computational findings suggesting that decreased DNA flexibility can lead to reduced UDG binding affinity by increasing the resistance of the DNA to adopt the bend enforced by protein binding (10). Increased structural rigidity introduced by pyrene is chemically reasonable because the extended  $\pi$  aromatic system of the pyrene base pair mimic is much more rigid than the native  $U^F \cdot A$  base pair which is only restrained by noncovalent hydrogen bonding. Assuming this interpretation for binding of the  $U^F \cdot Y$  base pair, its unfavorable rigidity is offset by the energetic benefit of extrahelical preorganization of the uracil. Thus, the binding affinity of  $U^F \cdot Y$  to UDG is similar to a  $U^F \cdot A$  base pair because of compensatory energetic effects, but  $U^F \cdot M$  binds more tightly because of the increased flexibility of the site (Table 2).

To further test the proposal that rigidity of the DNA has an adverse effect on UDG binding affinity, we tested the effect of the opposing base (A, M, or Y) on binding of DNA that contained an abasic site product analogue ( $\Phi$ ) (Table 2). Structural studies have shown that UDG can bind specifically to and flip out abasic sites to form a structurally indistinguishable complex as compared to substrate analogue DNA (2, 8, 37, 38). However, because there is no requirement for rupture of a base pair upon flipping of an abasic nucleotide, and there is no uracil attached to form hydrogen bonds and stacking interactions in the UDG active site, the changes in binding affinity between the  $\Phi \cdot Y$  and  $\Phi \cdot M$  duplexes should largely reflect differences in the intrinsic flexibility of the target site. As shown in Table 2,  $\Phi \cdot M$  binds ~480-fold more tightly than  $\Phi \cdot Y$  and 5-fold more tightly than  $\Phi \cdot A$ . The observed greater affinity of UDG for  $\Phi \cdot M$  over  $\Phi \cdot Y$  is identical to that of  $U^F \cdot M$  and  $U^F \cdot Y$  (Table 2). We conclude from these results that pyrene introduces an unfavorable free energy contribution to binding of as much as 3.7 kcal/mol arising from its increased rigidity and stacking as compared to sites that contain A or M as the opposing base. In conclusion, the observation that flexible abasic sites bind with much higher affinity than rigid abasic sites provides strong experimental evidence that specific recognition involves a flexibility component regardless of the presence of a uracil base.

## DISCUSSION

The mechanism by which enzymes obtain extraordinary specificity for their respective target sites in a large background of random DNA sequences has long been an active area of research. In this general area, DNA glycosylases have evolved a unique solution to this problem that is divergent from the sequence-dependent mechanisms of restriction enzymes, transcription factors, and repressor proteins. Obtaining a fundamental understanding of the kinetic and thermodynamic origins of DNA repair glycosylase specificity has the potential to allow rational targeting of these enzymes to engineered DNA sites that display features that promote enhanced binding and reactivity. Indeed, we have previously shown that simple rules derived from mechanistic studies of base flipping and catalysis can be used to alter UDG's specificity to recognize a cytosine base opposite to pyrene (i.e., a C $\cdot$ Y base pair) rather than uracil (39). Such findings offer the promise of altering the coding sequences of genes

in vivo using engineered glycosylases in combination with assisting targeting molecules such as pyrene-containing oligonucleotides.

**The Reaction Coordinate for Base Flipping.** It is difficult to imagine the pathway for flipping a base 180° from the DNA base stack ultimately leading to its precise docking into an enzyme active site. It is equally difficult to view how an enzyme could form specific interactions to guide a target base through a trajectory that arcs widely out of the DNA helix (Figure 1A) (7, 35). The present data suggest plausible mechanistic answers to these questions that are consistent with previous NMR dynamic and structural studies of the earliest steps in the base flipping process (7, 35) and also crystallographic studies of the final extrahelical complex (8).

To understand how an enzyme might facilitate the overall base flipping process, it is useful to consider the intrinsic kinetic and thermodynamic problems that must be overcome in extruding a base from the B DNA base stack (Figure 8). First, NMR imino proton exchange experiments have established that T•A, T•G, and U•A base pairs rapidly open at room temperature (7, 40, 41). These opening rates are greater than or equal to the rate constants for kinetic steps on the base flipping of UDG (Table 1), indicating that spontaneous base pair opening provides kinetically competent motions for seeding the enzymatic base flipping process. Indeed, recent studies of imino proton exchange of UDG-bound DNA have established that UDG does not alter the opening rate but instead substantially slows the closing rate constant of open T•A base pairs (7). This result is intuitively satisfying because the base pair closing rates in B DNA are exceedingly fast ( $\sim 10^7 \text{ s}^{-1}$ ) (42, 43), and one major problem in facilitating the migration of a base forward along the flipping trajectory is to prevent its retrograde motion back into the DNA base stack (Figure 8A). On the basis that adjacent T•A and G•C base pairs showed identical closing rates in the UDG complex ( $\sim 10^5 \text{ s}^{-1}$ ), but these rates differed by 25-fold in the free DNA, we proposed that UDG uses nonspecific DNA backbone interactions to increase the lifetime of a high-energy open state of the bound DNA that occurs very early on the flipping trajectory (**I**<sub>1</sub>, Figure 8A) (7). This open state of UDG-bound DNA is still extremely unstable and exists in dynamic equilibrium with closed B DNA. Nevertheless, the equilibrium is now shifted more toward the open state as compared to the free DNA (Figure 8A).

The next intermediate (**I**<sub>2</sub>) on the flipping pathway has an altered B DNA structure such that the uracil stacking interactions with the adjacent 2-AP are perturbed, but on average, the base pair hydrogen bonds are still intact (Figure 8A). The experimental observations that support these features of **I**<sub>2</sub> are (i) the rapid 2-AP fluorescence change indicating a perturbation in the stacking of uracil with 2-AP during the formation of **I**<sub>2</sub> (Figure 4A) and (ii) that the kinetic step between **I**<sub>2</sub> and the final extrahelical state (**P**) is kinetically enhanced as hydrogen bonds are removed from the U•X base pair (Figure 5C), indicating that these bonds persist after formation of **I**<sub>2</sub>. Once the final state is attained and the uracil is docked and held securely in the active site by stacking and hydrogen-bonding interactions (8, 38, 44–46), the extrahelical base cannot reenter the DNA stack without climbing the reverse activation barrier back to **I**<sub>2</sub>. Thus, the base flipping process may be viewed as the progressive formation of enzyme-bound states in which the

uracil base spends an ever increasing time in an extrahelical conformation as depicted in Figure 8A.

**The Importance of Being Flexible.** The kinetic and thermodynamic data indicate that as the base pair hydrogen bonds are removed, the second intermediate (**I**<sub>2</sub>), or the final extrahelical state (**P**), is increasingly stabilized (Figure 8B). The results also reveal that removal of the first two hydrogen bonds alters binding affinity by  $\sim 1 \text{ kcal/mol}$  per hydrogen bond but that removal of the final hydrogen bond results in a significantly larger 4 kcal/mol increase in the binding affinity (Figure 3B). Assuming that the base pair remains largely intact when the first two hydrogen bonds are broken, which is supported by both NMR and potassium permanganate oxidation sensitivity measurements (14, 47, 48), then the 1 kcal/mol free energy increment may provide an estimate of the individual hydrogen bond enthalpy (33). The free energy change when the last bond is removed is substantially greater than estimates of DNA base hydrogen bond energy (33, 49), indicating the loss of multiple energetic interactions, perhaps including stacking of the uracil with adjacent bases. We suggest that one ramification of total ablation of hydrogen bonds in the U<sup>F</sup>•X pair is increased conformational flexibility of the target site. Such conformational flexibility would be expected to facilitate DNA bending and, therefore, binding affinity. The conclusion that hydrogen bond ablation increases target site flexibility is further supported by the 3.7 kcal/mol unfavorable effect of the rigid pyrene (Y) nucleotide on binding as compared to 4-methylindole (M) when these nucleotides are placed opposite to uracil or an abasic site in duplex DNA (Table 2). We infer that pyrene, by forming strong stacking interactions and occupying a space that spans the width of the DNA duplex, significantly increases the resistance of the DNA toward bending, which is in turn reflected in the binding affinity measurements. Of course, the other destabilized base pairs may also exhibit changes in stacking energetics, but these differences are expected to be small given the very conservative changes in the nature of the opposing base (50). These differences in stacking energies, if present, would also be manifested in the flexibility of the DNA and would therefore contribute to the energetics of enzyme-induced DNA bending.

A free energy diagram depicting the significant effect of target site flexibility on binding is shown in Figure 8B. The diagram highlights how weaker U<sup>F</sup>•X base pairs are easier to bend due to their increased conformational flexibility, leading to a decrease in the free energy of the bent DNA, reflected in the stability of **I**<sub>2</sub> and **P** in Figure 8B.<sup>4</sup> In addition to the energetic benefit of increased flexibility of the U<sup>F</sup>•M substrate ( $\sim 3 \text{ kcal/mol}$ ), the **P** state realizes the additional energetic benefit of forming hydrogen bonds with the uracil base without the penalty of breaking hydrogen bonds in the base pair ( $\sim 3 \text{ kcal/mol}$ ).

The data uncover that a significant portion of UDG's intrinsic binding energy is used to drive the unfavorable process of DNA bending. Thus, a key question is the benefit

<sup>4</sup> This is similar to our previous conclusion that enthalpically destabilizing the uracil base pair promotes enhanced binding by increasing the probability of extrahelical states that are recognized by the enzyme (14). However, our previous interpretation did not include the effect of base pair flexibility on the energetics of DNA bending. Indeed, increased flexibility appears to be more important than the enthalpic benefit of removing hydrogen bonds.

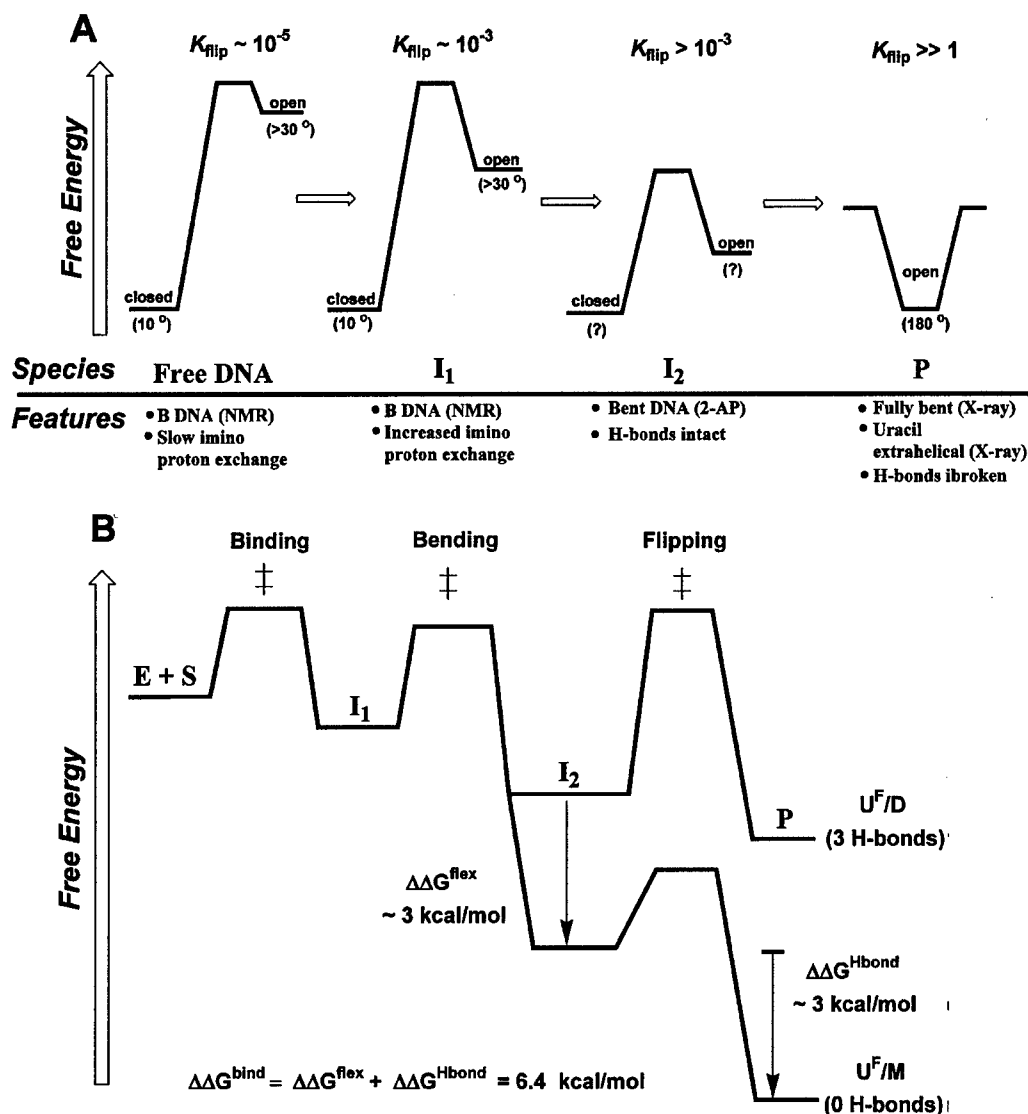


**FIGURE 8:** Free energy diagrams depicting the increasing base flipping equilibrium in each intermediate along the reaction coordinate for uracil flipping and the effect of base pair destabilization on binding affinity of UDG. (A) Free energy diagrams depicting the increasing equilibrium constant for uracil flipping along the reaction coordinate. The equilibrium,  $K_{flip} = [\text{open}]/[\text{closed}]$ , describes uracil in a closed, hydrogen-bonded state in the DNA duplex and an open state that is further along the reaction coordinate for base flipping. This flipping equilibrium is qualitatively depicted for the free DNA, the two enzyme-bound intermediates in Figure 1B ( $I_1$ ,  $I_2$ ), and the fully extrahelical product of the flipping reaction (P). The known structural and dynamic features of each depicted species are listed below each profile. The equilibrium constant  $K_{flip}$  has been measured for the free DNA ( $\sim 10^{-5}$ ) and for DNA bound in  $I_1$  ( $\sim 10^{-3}$ ) using NMR solvent magnetization transfer methods at 10 °C (7), establishing that UDG increases the equilibrium by about 100-fold in this early intermediate. Less is known about the structure of  $I_2$ , but the present results indicate DNA bending and largely intact base pair hydrogen bonds. In the P state, the uracil is held tightly in the active site, and the equilibrium is pushed all the way to the fully open state (180° rotation). Access to the closed state requires passage back over the transition state connecting  $I_2$  and P. The estimated rotation angles for the closed and open states are based on the pseudodihedral reaction coordinate defined by Banavali and MacKerell (11, 14), which ranges from 10° for uracil in B DNA to 180° for full rotation of the base out of the major groove. (B) Free energy effect of base pair destabilization on binding affinity of UDG ( $\Delta\Delta G^{bind} = \Delta\Delta G^{flex} + \Delta\Delta G^{Hbond}$ ). The relative free energy profiles for the stable  $U^F \cdot D$  duplex and the flexible  $U^F \cdot M$  duplex are depicted. The increased flexibility of the  $U^F \cdot M$  substrate decreases the free energy of  $I_2$  because less binding energy is required to bend the DNA at this step. The magnitude of the flexibility benefit is estimated as  $\Delta\Delta G^{flex} \sim 3 \text{ kcal/mol}$  (see text). In addition to the flexibility benefit, the absence of base pair hydrogen bonds in  $U^F \cdot M$  as compared to the three hydrogen bonds in  $U^F \cdot D$  enhances binding of the P state by  $\Delta\Delta G^{Hbond} \sim 3 \text{ kcal/mol}$  (see Figure 3B and text). This benefit arises because for  $U^F \cdot M$  there is no energetic price for breaking these bonds in the base pair. For simplicity we have shown that  $\Delta\Delta G^{flex}$  arises entirely at the  $I_2$  state, but this effect is more likely realized at both the  $I_2$  and P states.

derived from this significant energetic expenditure. Since the rate of spontaneous base pair opening is already fast compared to events on the base flipping pathway, it is mechanistically reasonable to propose that the role of enzyme-induced DNA bending is to promote forward commitment along the pathway rather than to lower activation barriers to flipping (i.e., stabilization of extrahelical intermediates).<sup>5</sup>

UDG likely promotes forward migration of the uracil down the pathway by forming nonspecific interactions with the

<sup>5</sup> Computational studies on UDG and other enzymes have suggested that DNA bending facilitates base flipping (9–12, 51–55), and a recent computational study on HhaI (cytosine-C5)-methyltransferase indicates that this enzyme acts by forming a web of interactions with several high-energy intermediates along the flipping pathway (56).

DNA backbone which become progressively stronger during the formation of two discrete intermediates ( $I_1$  and  $I_2$ , Figure 1B). In the earliest nonspecific intermediate ( $I_1$ ), NMR imino exchange experiments indicate that UDG increases the opening equilibrium ([open]/[closed]) by almost 100-fold (2.8 kcal/mol), largely by decreasing the closing rate (7). In the subsequent intermediate ( $I_2$ ), the magnitude of the equilibrium is currently unknown, but a further increase is suggested because the uracil has substantially decreased stacking interactions with the adjacent 2-AP base arising from DNA bending. Since the presence of uracil is required to achieve  $I_2$ , then this intermediate must be considered a specific complex in which the enzyme recognizes some feature of the uracil base. The extent or nature of the discrimination between uracil and other normal DNA bases at this intermediate step is currently not known. In conclusion, our view based on these findings is that UDG facilitates base flipping by utilizing binding energy to alter the DNA structure, thereby progressively shifting the flipping equilibrium toward the open state that is ultimately trapped by specific interactions located within the uracil binding pocket. The specific interactions are formed only very late in the process, and thus, the earlier steps in the flipping pathway are largely driven by nonspecific interactions. A further experimental goal with UDG is to unambiguously identify the amino acid side chains that promote the stepwise transition from the closed to open state.

**Conclusion.** We have uncovered the origins of high-affinity binding of UDG to an extrahelical uracil base. By discretely altering base pair hydrogen bonding and site flexibility, we have found that high binding affinity is determined more by the flexibility of the site than by the enthalpic benefit of removing base pair hydrogen bonds. Thus a significant contribution to enzymatic base flipping is the unfavorable energetic cost of DNA bending. This cost is estimated in two ways: (i) the stiffening effect of pyrene (3.7 kcal/mol) and (ii) the additional favorable energetic effect on binding of removing the last hydrogen bond from the uracil base pair (~3 kcal/mol). In the future, these simple features of high-affinity target site binding by UDG may be utilized to direct UDG to specific sites in genomic DNA.

## REFERENCES

- Stivers, J. T., and Jiang, Y. L. (2003) A mechanistic perspective on the chemistry of DNA repair glycosylases, *Chem. Rev.* **103**, 2729–2759.
- Parikh, S. S., Mol, C. D., Slupphaug, G., Bharati, S., Krokan, H. E., and Tainer, J. A. (1998) Base excision repair initiation revealed by crystal structures and binding kinetics of human uracil-DNA glycosylase with DNA, *EMBO J.* **17**, 5214–5226.
- Slupphaug, G., Mol, C. D., Kavli, B., Arvai, A. S., Krokan, H. E., and Tainer, J. A. (1996) A nucleotide-flipping mechanism from the structure of human uracil-DNA glycosylase bound to DNA, *Nature* **384**, 87–92.
- Stivers, J. T. (2004) Site-specific DNA damage recognition by enzyme-induced base flipping, *Prog. Nucleic Acid Res. Mol. Biol.* **77**, 37–65.
- Stivers, J. T., Pankiewicz, K. W., and Watanabe, K. A. (1999) Kinetic mechanism of damage site recognition and uracil flipping by *Escherichia coli* uracil DNA glycosylase, *Biochemistry* **38**, 952–963.
- Jiang, Y. L., and Stivers, J. T. (2002) Mutational analysis of the base flipping mechanism of uracil DNA glycosylase, *Biochemistry* **41**, 11236–11247.
- Cao, C., Jiang, Y. L., Stivers, J. T., and Song, F. (2004) Dynamic opening of DNA during the enzymatic search for a damaged base, *Nat. Struct. Mol. Biol.* **11**, 1230–1236.
- Parikh, S. S., Walcher, G., Jones, G. D., Slupphaug, G., Krokan, H. E., Blackburn, G. M., and Tainer, J. A. (2000) Uracil-DNA glycosylase-DNA substrate and product structures: Conformational strain promotes catalytic efficiency by coupled stereoelectronic effects, *Proc. Natl. Acad. Sci. U.S.A.* **97**, 5083–5088.
- Fuxreiter, M., Luo, N., Jedlovsky, P., Simon, I., and Osman, R. (2002) Role of base flipping in specific recognition of damaged DNA by repair enzymes, *J. Mol. Biol.* **323**, 823–834.
- Seibert, E., Ross, J. B., and Osman, R. (2002) Role of DNA flexibility in sequence-dependent activity of uracil DNA glycosylase, *Biochemistry* **41**, 10976–10984.
- Banavali, N. K., and MacKerell, A. D., Jr. (2002) Free energy and structural pathways of base flipping in a DNA gcgc containing sequence, *J. Mol. Biol.* **319**, 141–160.
- Huang, N., Banavali, N. K., and MacKerell, A. D., Jr. (2003) Protein-facilitated base flipping in DNA by cytosine-5-methyltransferase, *Proc. Natl. Acad. Sci. U.S.A.* **100**, 68–73.
- Jencks, W. P. (1985) A primer for the bema hapothole—an empirical approach to the characterization of changing transition-state structures, *Chem. Rev.* **85**, 511–527.
- Krosky, D. J., Schwarz, F. P., and Stivers, J. T. (2004) Linear free energy correlations for enzymatic base flipping: How do damaged base pairs facilitate specific recognition?, *Biochemistry* **43**, 4188–4195.
- Rachofsky, E. L., Osman, R., and Ross, J. B. (2001) Probing structure and dynamics of DNA with 2-aminopurine: Effects of local environment on fluorescence, *Biochemistry* **40**, 946–956.
- Rachofsky, E. L., Seibert, E., Stivers, J. T., Osman, R., and Ross, J. B. (2001) Conformation and dynamics of abasic sites in DNA investigated by time-resolved fluorescence of 2-aminopurine, *Biochemistry* **40**, 957–967.
- Jiang, Y. L., Song, F., and Stivers, J. T. (2002) Base flipping mutations of uracil DNA glycosylase: Substrate rescue using a pyrene nucleotide wedge, *Biochemistry* **41**, 11248–11254.
- Gowher, H., and Jeltsch, A. (2000) Molecular enzymology of the ecorv DNA-(adenine-n(6))-methyltransferase: Kinetics of DNA binding and bending, kinetic mechanism and linear diffusion of the enzyme on DNA, *J. Mol. Biol.* **303**, 93–110.
- Su, T. J., Connolly, B. A., Darlington, C., Mallin, R., and Dryden, D. T. (2004) Unusual 2-aminopurine fluorescence from a complex of DNA and the ecoli methyltransferase, *Nucleic Acids Res.* **32**, 2223–2230.
- Wong, I., Lundquist, A. J., Bernards, A. S., and Mosbaugh, D. W. (2002) Presteady-state analysis of a single catalytic turnover by *Escherichia coli* uracil-DNA glycosylase reveals a “pinch-pull-push” mechanism, *J. Biol. Chem.* **277**, 20.
- Vallur, A. C., Feller, J. A., Abner, C. W., Tran, R. K., and Bloom, L. B. (2002) Effects of hydrogen bonding within a damaged base pair on the activity of wild type and DNA-intercalating mutants of human alkyladenine DNA glycosylase, *J. Biol. Chem.* **277**, 31673–31678.
- Liu, P., Burdzy, A., and Sowers, L. C. (2002) Substrate recognition by a family of uracil-DNA glycosylases: Ung, mug, and tdg, *Chem. Res. Toxicol.* **15**, 1001–1009.
- Valinluck, V., Liu, P., Burdzy, A., Ryu, J., and Sowers, L. C. (2002) Influence of local duplex stability and n(6)-methyladenine on uracil recognition by mismatch-specific uracil-DNA glycosylase (mug), *Chem. Res. Toxicol.* **15**, 1595–1601.
- Biswas, T., Clos, L. J., II, SantaLucia, J., Jr., Mitra, S., and Roy, R. (2002) Binding of specific DNA base-pair mismatches by n-methylpurine-DNA glycosylase and its implication in initial damage recognition, *J. Mol. Biol.* **320**, 503–513.
- Chepanoske, C. L., Langelier, C. R., Chmiel, N. H., and David, S. S. (2000) Recognition of the nonpolar base 4-methylindole in DNA by the DNA repair adenine glycosylase muty, *Org. Lett.* **2**, 1341–1344.
- O’Brien, P. J., and Ellenberger, T. (2004) The *Escherichia coli* 3-methyladenine DNA glycosylase alkA has a remarkably versatile active site, *J. Biol. Chem.* **279**, 26876–26884.
- O’Brien, P. J., and Ellenberger, T. (2004) Dissecting the broad substrate specificity of human 3-methyladenine-DNA glycosylase, *J. Biol. Chem.* **279**, 9750–9757.
- Daniels, D. S., Woo, T. T., Luu, K. X., Noll, D. M., Clarke, N. D., Pegg, A. E., and Tainer, J. A. (2004) DNA binding and nucleotide flipping by the human DNA repair protein agt, *Nat. Struct. Mol. Biol.* **11**, 714–720.
- Moran, S., Ren, R. X. F., Sheils, C. J., Rumney, S., and Kool, E. T. (1996) Non-hydrogen bonding “terminator” nucleosides in-

- crease the 3'-end homogeneity of enzymatic RNA and DNA synthesis, *Nucleic Acids Res.* 24, 2044–2052.
30. Ren, R. X. F., Chaudhuri, N. C., Paris, P. L., Rumney, S., and Kool, E. T. (1996) Naphthalene, phenanthrene, and pyrene as DNA base analogues: Synthesis, structure, and fluorescence in DNA, *J. Am. Chem. Soc.* 118, 7671–7678.
31. Fasman, G. D. (1975) *Handbook of biochemistry and molecular biology: Nucleic acids*, Vol. 1, 3rd ed., CRC Press, Boca Raton, FL.
32. Drohat, A. C., Jagadeesh, J., Ferguson, E., and Stivers, J. T. (1999) Role of electrophilic and general base catalysis in the mechanism of *Escherichia coli* uracil DNA glycosylase, *Biochemistry* 38, 11866–11875.
33. Turner, D. H., Sugimoto, N., Kierzek, R., and Dreiker, S. D. (1987) Free-energy increments for hydrogen-bonds in nucleic-acid base-pairs, *J. Am. Chem. Soc.* 109, 3783–3785.
34. Jiang, Y. L., Kwon, K., and Stivers, J. T. (2001) Turning on uracil-DNA glycosylase using a pyrene nucleotide switch, *J. Biol. Chem.* 276, 42347–42354.
35. Jiang, Y. L., McDowell, L. M., Poliks, B., Studelska, D. R., Cao, C., Potter, G. S., Schaefer, J., Song, F., and Stivers, J. T. (2004) Recognition of an unnatural difluorophenyl nucleotide by uracil DNA glycosylase, *Biochemistry* 43, 15429–15438.
36. Matray, T. J., and Kool, E. T. (1999) A specific partner for abasic damage in DNA, *Nature* 399, 704–708.
37. Bianchet, M. A., Seiple, L. A., Jiang, Y. L., Ichikawa, Y., Amzel, L. M., and Stivers, J. T. (2003) Electrostatic guidance of glycosyl cation migration along the reaction coordinate of uracil DNA glycosylase, *Biochemistry* 42, 12455–12460.
38. Werner, R. M., Jiang, Y. L., Gordley, R. G., Jagadeesh, G. J., Ladner, J. E., Xiao, G., Tordova, M., Gilliland, G. L., and Stivers, J. T. (2000) Stressing-out DNA? The contribution of serine-phosphodiester interactions in catalysis by uracil DNA glycosylase, *Biochemistry* 39, 12585–12594.
39. Kwon, K., Jiang, Y., and Stivers, J. (2003) Rational engineering of a DNA glycosylase specific for an unnatural cytosine:pyrene base pair, *Chem. Biol.* 10, 1–20.
40. Moe, J. G., and Russu, I. M. (1992) Kinetics and energetics of base-pair opening in 5'-d(cgcgaattcgcg)-3' and a substituted dodecamer containing g.T mismatches, *Biochemistry* 31, 8421–8428.
41. Moe, J. G., and Russu, I. M. (1990) Proton exchange and base pair opening kinetics in 5'-d(cgcgaattcgcg)-3' and related dodecamers, *Nucleic Acids Res.* 18, 821–827.
42. Gueron, M., Charretier, E., Hagerhorst, J., Kochoyan, M., Leroy, J. L., and Moraillon, A. (1990) in *Structural methods* (Sarma, R. H., Ed.) pp 113–137, Adenine Press, New York.
43. Gueron, M., and Leroy, J.-L. (1995) Studies of base pair kinetics by NMR measurement of proton exchange, *Methods Enzymol.* 261, 383–413.
44. Dong, J., Drohat, A. C., Stivers, J. T., Pankiewicz, K. W., and Carey, P. R. (2000) Raman spectroscopy of uracil DNA glycosylase-DNA complexes: Insights into DNA damage recognition and catalysis, *Biochemistry* 39, 13241.
45. Drohat, A. C., and Stivers, J. T. (2000) NMR evidence for an unusually low  $n_1$  pKa for uracil bound to uracil DNA glycosylase: Implications for catalysis, *J. Am. Chem. Soc.* 122, 1840–1841.
46. Drohat, A. C., Xiao, G., Tordova, M., Jagadeesh, J., Pankiewicz, K. W., Watanabe, K. A., Gilliland, G. L., and Stivers, J. T. (1999) Heteronuclear NMR and crystallographic studies of wild-type and h187q *Escherichia coli* uracil DNA glycosylase: Electrophilic catalysis of uracil expulsion by a neutral histidine 187, *Biochemistry* 38, 11876–11886.
47. Ikuta, S., Eritja, R., Kaplan, B. E., and Itakura, K. (1987) NMR studies of the stable mismatch purine-thymine in the self-complementary d(cgpuaatttcg) duplex in solution, *Biochemistry* 26, 5646–5650.
48. Clore, G. M., Oschkinat, H., McLaughlin, L. W., Benseler, F., Happ, C. S., Happ, E., and Gronenborn, A. M. (1988) Refinement of the solution structure of the DNA dodecamer 5'-d(cgcgpatcgcg)-2' containing a stable purine-thymine base pair: Combined use of nuclear magnetic resonance and restrained molecular dynamics, *Biochemistry* 27, 4185–4197.
49. Freier, S. M., Kierzek, R., Caruthers, M. H., Neilson, T., and Turner, D. H. (1986) Free-energy contributions of g.U and other terminal mismatches to helix stability, *Biochemistry* 25, 3209–3213.
50. Guckian, K. M., Schweitzer, B. A., Ren, R. X. F., Sheils, C. J., Tahmassebi, D. C., and Kool, E. T. (2000) Factors contributing to aromatic stacking in water: Evaluation in the context of DNA, *J. Am. Chem. Soc.* 122, 2213–2222.
51. Clegg, R. M., Murchie, A. I., Zechel, A., Carlberg, C., Diekmann, S., and Lilley, D. M. (1992) Fluorescence resonance energy transfer analysis of the structure of the four-way DNA junction, *Biochemistry* 31, 4846–4856.
52. Hiller, D. A., Fogg, J. M., Martin, A. M., Beechem, J. M., Reich, N. O., and Perona, J. J. (2003) Simultaneous DNA binding and bending by *ecorv* endonuclease observed by real-time fluorescence, *Biochemistry* 42, 14375–14385.
53. Lorenz, M., Hillisch, A., Goodman, S. D., and Diekmann, S. (1999) Global structure similarities of intact and nicked DNA complexed with *ihf* measured in solution by fluorescence resonance energy transfer, *Nucleic Acids Res.* 27, 4619–4625.
54. Vamosi, G., Gohlke, C., and Clegg, R. M. (1996) Fluorescence characteristics of 5-carboxytetramethylrhodamine linked covalently to the 5' end of oligonucleotides: Multiple conformers of single-stranded and double-stranded dye-DNA complexes, *Biophys. J.* 71, 972–994.
55. Hopkins, B. B., and Reich, N. O. (2004) Simultaneous DNA binding, bending, and base flipping: Evidence for a novel *m.EcoRI* methyltransferase-DNA complex, *J. Biol. Chem.* 279, 37049–37060.
56. Huang, N., and MacKerell, A. D., Jr. (2005) Specificity in protein-DNA interactions: Energetic recognition by the (cytosine-c5)-methyltransferase from *hhai*, *J. Mol. Biol.* 345, 265–274.
57. Cheong, C., Tinoco, I., Jr., and Chollet, A. (1988) Thermodynamic studies of base pairing involving 2,6-diaminopurine, *Nucleic Acids Res.* 16, 5115–5122.
58. Chazin, W. J., Rance, M., Chollet, A., and Leupin, W. (1991) Comparative NMR analysis of the decaoxynucleotide d-(gcattaatgc)-2' and an analogue containing 2-aminoadenine, *Nucleic Acids Res.* 19, 5507–5513.
59. Carbonnaux, C., Fazakerley, G. V., and Sowers, L. C. (1990) An NMR structural study of deaminated base pairs in DNA, *Nucleic Acids Res.* 18, 4075–4081.

BI050084U